

# Influence of Sparger Type and Regime of Fluid on Biomass and Lipid Productivity of *Chlorella vulgaris* Culture in a Pilot Airlift Photobioreactor



This work is licensed under a Creative Commons Attribution 4.0 International License

Y. López-Hernández,<sup>a</sup> C. Orozco,<sup>a</sup> I. García-Peña,<sup>a</sup> J. Ramírez-Muñoz,<sup>b</sup> and L. G. Torres<sup>a,\*</sup>

<sup>a</sup>Bioprosesos, UPIBI-Instituto Politécnico Nacional, Acueducto s/n, C.P. 07340, Del. Gustavo A Madero, Mexico City, Mexico

<sup>b</sup>Departamento de Energía, Universidad Autónoma Metropolitana-Azcapotzalco, Mexico City, Mexico

doi: 10.15255/CABEQ.2018.1403

Original scientific paper

Received: June 6, 2018

Accepted: March 9, 2018

The effect of different types of spargers and the influence of the air flow rate on biomass and lipids production by *Chlorella vulgaris* was evaluated. These data allowed correlation of the hydrodynamic behavior of the photobioreactor with the byproducts production. The hydrodynamic characterization was developed by determining the mixing time ( $t_M$ ), hold-up, and total volumetric mass transfer coefficient of  $\text{CO}_2$ ,  $k_L a(\text{CO}_2)_T$ , at increasing air flow rates for three different spargers: star-shaped, cross-shaped and porous glass surface sparger. The hydrodynamic characterization showed that the  $t_M$  decreased, while the hold-up values and the  $k_L a(\text{CO}_2)_T$  increased as a result of the increment in the volumetric air flow rate between 5 to 17  $\text{L min}^{-1}$ . The highest biomass and lipid concentrations were determined at the higher aeration rate (20  $\text{L min}^{-1}$ ), which was correlated with the lower  $t_M$ , the higher hold-up and  $k_L a(\text{CO}_2)_T$  values. Biomass and lipid production showed an inverse correlation. The highest biomass concentration (750  $\text{mg L}^{-1}$ ) and the lowest lipid concentration (10  $\text{mg L}^{-1}$ ) were measured with the star sparger. In contrast, when the lowest biomass concentration was obtained (240  $\text{mg L}^{-1}$ ), the highest lipid concentration of 196  $\text{mg L}^{-1}$  was measured with the glass sparger. The maximum biomass productivity values were determined at the lower aeration rate and the star sparger, with the minimum power per unit of volume, which could be useful for a cost-effective process.

## Keywords:

aeration regime, airlift photobioreactor, *Chlorella vulgaris*, hydrodynamic characterization, microalgae, lipids

## Introduction

Photobioreactors (PBR) have been designed and developed at laboratory and pilot plant scales since the 1950s. Several configurations have been suggested, including tubular, flat plate, bubble column, and airlift<sup>1</sup>. Ultimately, the final configuration should rely on the microorganism and the products to be recovered. For instance, the use of airlift systems for microalgae and lipid production is recommended<sup>2–6</sup> because of the relatively low energy requirements and the homogeneous distribution of hydrodynamic shear<sup>7</sup>.

The PBR operating conditions have a direct effect on the biomass and lipids production. Final bio-

mass yield and lipid content are the result of the combined effect of biological factors (type of culture/strain, culture conditions, culture density, concentration of  $\text{CO}_2$ , and  $\text{O}_2$  accumulation), and physical factors (mass transfer, fluid dynamics and irradiance). Some physical factors, such as the mixing efficiency, influence the mass transfer as do light and substrate availability, which have a strong effect on the biological process. Light availability is a key factor in the photosynthetic process; light is absorbed and scattered by the cells<sup>8</sup>; therefore, it has an effect on the specific growth rate, and consequently, on the biomass productivity.

The hydrodynamics in the PBR for some configurations could be determined by the type of sparger and will define the spatial light distribution<sup>9</sup>. Light distribution becomes critical at a certain biomass concentration, and then it is necessary to ensure that the cells are exposed to the same light

\*Corresponding author: Dr. Luis G. Torres (lgtorresbustillos@gmail.com)

incidence. In bubble column devices (e.g., airlift PBR), the sparger type and the air flow rate affect the hydrodynamic interaction. The hydrodynamic interaction influences drastically the breaking and coalescence processes, affecting the bubbles size distribution, i.e., the total area available for contact between phases (interfacial area), and the velocity of bubbles (residence time for interfacial contact). Consequently, it contributes to the performance of the equipment, and therefore, the hydrodynamic characterization is necessary either to improve the performance of existing devices or to obtain fundamental information for scaling and design<sup>10,11</sup>. New PBR designs allow more efficient light use, with less energy consumption, and adequate mass transfer rates for photosynthetic biomass production. Mass transfer rates in a bioreactor are largely affected by the fluid properties, liquid and gas velocity, and by the geometry and type of bioreactor. Mass transfer is frequently assessed by the volumetric mass transfer coefficient ( $k_L a$ ). In practical terms, prediction and optimization of mass transfer by  $k_L a$  will maximize the mass transfer with minimal energy input<sup>12</sup>.

Some authors<sup>2–4,6,13</sup> have performed the hydrodynamic characterization of different types of reactors (STR, parallel plate, airlift systems) and correlated mixing times,  $k_L a$  values, and other parameters with the microalgae growth rates of specific strains, and, in very few cases, with lipid production. As reported by Reyna-Velarde *et al.*<sup>2</sup>, the flat-plate bioreactor (FPBR) has been designed for the optimal use of light<sup>14–16</sup>. In their work<sup>2</sup>, the authors demonstrated the effect of superficial gas velocity ( $U_g$ ) on the volumetric mass transfer coefficient ( $k_L a$ ), the gas hold-up ( $\epsilon$ ), and the mixing time ( $t_M$ ) in a PBR with a culture of *Spirulina* sp. The data demonstrated that at  $U_g$  values above  $4.2 \cdot 10^{-3}$  m s<sup>-1</sup>, no substantial increase in mass transfer was observed, even when the air flow had been increased. This indicated that, at such  $U_g$ , bubble coalescence increased probably due to an increase in the bubble number within the fluid<sup>12,17</sup> which favored bubble collision and probably caused a decrease in the interfacial area value ( $a$ ) for mass transfer, preventing an increase in  $k_L a$ . Kumar and Das<sup>3</sup> reported a comparative analysis of an airlift and bubble column based on the growth kinetic, mixing time, and volumetric mass transfer coefficient. These reactors were evaluated for CO<sub>2</sub> sequestering and concomitant algae biomass production. The biomass production was higher in the airlift compared to the bubble column; the authors attributed this fact to a lower velocity of culture movement in the downcomer (light zone of the reactor) as it ensured better light exposure to the algal

cells. On the other hand,  $k_L a$  of the bubble column reactor was distributed better than in the airlift reactor. Great differences in  $k_L a$  values of the central draft tube and the annular region were determined. The  $k_L a$  was lower in the annular region compared to central draft tube region of the airlift reactor, meaning that, at the annular region, it took a long time to become saturated with dissolved oxygen. In general, Kumar and Das<sup>3</sup> determined that  $k_L a$  values were higher in the bubble column than in the central draft tube region of the airlift reactor. This behavior was not expected because the central draft tube of the airlift reactor behaved like a bubble column reactor, therefore  $k_L a$  values might be similar. The authors suggested that this effect could be attributed to larger sized bubbles and higher superficial gas velocity in the draft tube as compared to the bubble column reactor. Larger sized bubbles decrease the interfacial area of gas and liquid as well as the retention time because of high bubble rise velocities. Other authors, like Shamlou *et al.*<sup>18</sup>, found a lower value of  $k_L a$  only at the lower portion of the downcomer, while the upper portion had higher  $k_L a$  value. Finally, Rengel<sup>4</sup> proposed a model for airlift reactor where the variation of air bubble velocity, as an effect of variations in the volumetric air flow rate, was evaluated. Data obtained in that study showed a relationship between riser and downcomer gas hold-ups; additionally, it was shown that liquid velocities increase with volumetric air flow rate. Liquid circulation time found in each section of the reactor was similar of those typically employed in microalgae culture.

In recent years, there is a growing interest for the optimal design of photobioreactor (PBR) that meets the requirements of photosynthetic microorganisms to increase the low production efficiency in large-scale microalgal processes. However, many engineering problems have yet to be solved in order to develop low-cost efficient systems at an industrial scale<sup>2</sup>. The need to study and determine the hydrodynamic behavior of the PBR before its use in microalgae productions, and the determination of the biological and physical phenomena allows to model, simulate, and enhance the algal productivities (biomass and lipids production). Therefore, the goals of this study were three: 1) hydrodynamic characterization of a 17-L airlift bioreactor using different aeration rates and types of spargers, including the calculation of the gas-liquid mass transfer coefficient of CO<sub>2</sub>,  $k_L a(\text{CO}_2)_T$ ; 2) to assess the effect of the three spargers and of the air flow rate on the biomass and lipid production by *Chlorella vulgaris*; and 3) to correlate the results with the hydrodynamic characteristics of the PBR.

## Materials and methods

### Photobioreactor and spargers

The experiments were carried out in a 17-L glass airlift divided into three sections, all of them jointed by Teflon lips and adjusted with screws. The PBR had two sample ports inside the reactor for pH or dissolved oxygen electrodes, and at the bottom of the first module (see Fig. 1). Another sample port was located at the bottom of module 1, where the specific sparger was connected. The riser section/downcomer section ratio,  $A_r/A_d$ , of the airlift was 0.419. The bottom clearance was of 0.06 m, and the total liquid and reactor capacities were 17.0 and 17.5 L, respectively. The external cylinder had internal and external diameters of 0.17 and 0.18 m, respectively. Finally, the draft tube had internal and external diameters of 0.089 and 0.1 m, with areas of 0.006 and 0.023 m<sup>2</sup>, respectively. Fig. 1 shows the airlift photobioreactor, together with the three air spargers.

Three different spargers were used: one made of glass with a porous glass surface, and two made of stainless steel in the shape of a cross (four cylindrical elements), and a star (six cylindrical elements). The cylindrical elements had perforations of 0.00 m diameter, separated by 0.002 m. The total

diameters of the star and cross spargers were 0.08 m, while the glass sparger had a diameter of 0.06 m, and the reported diameter of the holes was about 100 to 160  $\mu\text{m}$  (Fig. 1).

The airlift was equipped with six fluorescent lamps and LED stripes, as shown in Fig. 1. The irradiation received at the center of the riser glass tube was, in average, 100  $\mu\text{mol}$  of photons  $\text{m}^{-2} \text{s}^{-1}$  (or  $\mu\text{E m}^{-2} \text{s}^{-1}$ ). This value was calculated as follows: six points of an imaginary plane were distributed radially on the top, middle, and bottom of the airlift. In those points, the irradiation was measured using a PAR Quantum system (Skye, USA), and all 18 values were averaged. The airlift was placed inside a room where the average temperature during the day was about  $20 \pm 2$  °C. A rotameter model 054-17 with a free-flowing stainless steel sphere was used to measure and regulate the flow of air from the compressor. Air flow values for hydrodynamic tests were 5, 9, 14, 17, and 20  $\text{L min}^{-1}$ . Tap water was used for all hydrodynamic testing, except for determining the volumetric flow rate of mass transfer, which was determined in bold basal medium (BBM).

The BBM was prepared by dissolving the following salts in water (amounts in  $\text{g L}^{-1}$ ):  $\text{NaNO}_3$  (0.250);  $\text{MgSO}_4 \cdot 7\text{H}_2\text{O}$  (0.075);  $\text{CaCl}_2$  (0.025);  $\text{NaCl}$  (0.025);  $\text{FeSO}_4 \cdot 7\text{H}_2\text{O}$  (0.00498); EDTA (0.05);  $\text{KOH}$  (0.031);  $\text{K}_2\text{HPO}_4$  (0.07);  $\text{KH}_2\text{PO}_4$  (0.175). Trace amounts of the following compounds were also added:  $\text{H}_3\text{BO}_3$  (0.01142);  $\text{ZnSO}_4 \cdot 7\text{H}_2\text{O}$  (0.00882);  $\text{MnCl}_2 \cdot 4\text{H}_2\text{O}$  (0.00144);  $\text{Na}_2\text{MoO}_4$  (0.0011975);  $\text{CuSO}_4 \cdot 5\text{H}_2\text{O}$  (0.00157);  $\text{Co}(\text{NO}_3)_2$  (0.00049).

### Hydrodynamic variables

#### Hold up

Hold up ( $\varepsilon$ ) was evaluated using the method of volumetric expansion<sup>19</sup> by the height difference of the liquid with and without aeration (Eq. 1):

$$\varepsilon = \frac{H_G - H_L}{H_G} \quad (1)$$

where  $H_G$  and  $H_L$  are gassed liquid height (m) and height of still liquid without aerating (m), respectively. Hold-up values with the three spargers shown in Fig. 1 were determined for five air flows: 5, 9, 14, 17, and 20  $\text{L min}^{-1}$ .

#### Mixing time

The mixing time was determined by measuring pH changes at given time intervals. The three different spargers with an air flow of 5  $\text{L min}^{-1}$  were used to promote the mixing of the liquid. A pulse of 10 mL of a NaOH solution at a concentration of

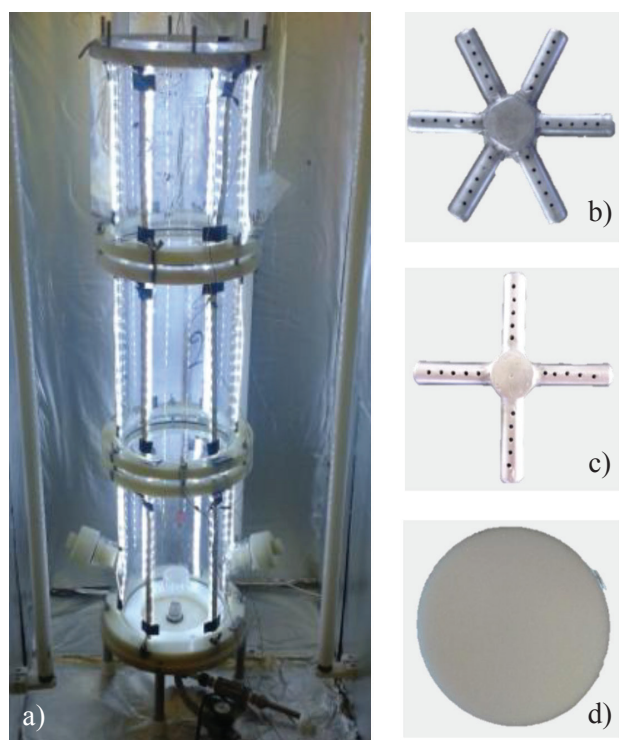


Fig. 1 – a) Photobioreactor and the three different spargers employed in this work: b) star type; c) cross type; and d) porous glass sparger

200 g L<sup>-1</sup> was then added to the operating volume of the reactor in the top liquid surface. A Thermo Scientific Model 8102BNUWP potentiometer was used for measuring pH changes. It remained in the same position, and a pulse of a NaOH solution at a concentration of 200 g L<sup>-1</sup> was injected into the reactor until a stable pH in the volume of water inside the reactor was reached. Finally, pH changes were recorded every second and normalized, and the mixing times to attain 99 % of the pH final values were consolidated. This process was performed in duplicate for the different aeration rates (5, 9, 14, 17, and 20 L min<sup>-1</sup>).

The specific power input ( $P_g/V$ ) in W m<sup>-3</sup>, defined as the power supplied by the gas per unit volume of fluid, and which is due to isothermal expansion through the height of the riser<sup>4,20</sup>, was calculated by means of Eq. 2:

$$P_g/V = \frac{Q_m RT}{V_L} \ln \left( 1 + \frac{\rho g H}{p_a} \right) \quad (2)$$

where  $Q_m$  is the molar flow of air (mol s<sup>-1</sup>),  $R$  is the gas constant (8.314 J mol<sup>-1</sup> K<sup>-1</sup>),  $T$  is the temperature (293.15 K),  $V_L$  is the operating volume of the reactor (0.017 m<sup>3</sup>),  $\rho$  and  $g$  are the density of water (at 20 °C, 998.29 kg m<sup>-3</sup>) and acceleration of gravity (9.81 m s<sup>-2</sup>), respectively.  $H$  is the height of liquid unaerated (0.7490 m) and  $p_a$  is the head pressure (atmospheric pressure for Mexico City, 7.80 · 10<sup>4</sup> Pa).

$k_L a$  values for O<sub>2</sub> and CO<sub>2</sub>

The volumetric mass transfer coefficient ( $k_L a$ ) was determined by displacing the oxygen (O<sub>2</sub>) contained in the BBM<sup>21</sup>. An Oakton Series 300 O<sub>2</sub> sensor was used for the measurement of dissolved oxygen. The sensor was placed inside one of the ports of the reactor (downcomer zone). By using the cross sparger, inert gas, nitrogen (N<sub>2</sub>), was bubbled in the same medium until a concentration of 0.7 mg L<sup>-1</sup> of dissolved oxygen was reached. At this concentration of oxygen in the BBM, nitrogen injection was stopped and the introduction of air from a compressor at a volumetric flow of 5 L min<sup>-1</sup> was started. Dissolved oxygen changes were recorded from 0.7 ppm every 20 seconds until stability was reached. Collected data were fitted to Eq. 3.

$$\ln \left( \frac{\gamma^* - \gamma_0}{\gamma^* - \gamma} \right) = k_L a(O_2)(t - t_0) \quad (3)$$

In this equation, the slope corresponds to the volumetric mass transfer coefficient  $k_L a(O_2)$ ,  $\gamma^*$  is the saturation concentration of dissolved oxygen,  $\gamma_0$  is the dissolved oxygen concentration at zero time ( $t_0$ ),

and  $\gamma$  is the concentration of dissolved oxygen at a given time ( $t$ ).  $k_L a(O_2)$  was also calculated for the area riser with the same sensor and technique as described previously. Likewise,  $k_L a$  for the remaining two spargers, i.e., star-type sparger and porous glass sparger, was calculated using the same technique. All tests were performed in duplicate for five aeration flows: 5, 9, 14, 17, and 20 L min<sup>-1</sup>. Values for  $k_L a(CO_2)$  were obtained by the equation relating  $k_L a$  of oxygen and the ratio of the diffusion coefficients of oxygen and CO<sub>2</sub>, see Eq. 4<sup>22</sup>.

$$k_L a(CO_2) = \sqrt{\frac{D_{O_2}}{D_{CO_2}}} k_L a(O_2) \quad (4)$$

where  $k_L a(CO_2)$  and  $k_L a$  are volumetric mass transfer coefficient of CO<sub>2</sub> (h<sup>-1</sup>) and volumetric mass transfer coefficient of O<sub>2</sub> (h<sup>-1</sup>), respectively.  $D_{O_2}$  and  $D_{CO_2}$  are oxygen diffusion coefficient at 20 °C (1.22 · 10<sup>-10</sup> m s<sup>-2</sup>) and diffusion coefficient of carbon dioxide at 20 °C (1.76 · 10<sup>-9</sup> m s<sup>-2</sup>), respectively

With Eq. 5, where T is the total volumetric mass transfer coefficient of CO<sub>2</sub>,  $k_L a(CO_2)_T$  involving the riser and downcomer zones, found by the ratio of the areas of the cross sections of each zone, was calculated:

$$k_L a(CO_2)_T = \frac{A_r k_L a_r + A_d k_L a_d}{A_r + A_d} \quad (5)$$

where  $k_L a(CO_2)_T$  is total volumetric mass transfer coefficient of CO<sub>2</sub> (h<sup>-1</sup>).  $k_L a_r$  and  $k_L a_d$  are volumetric mass transfer coefficients for the riser (h<sup>-1</sup>) and the downcomer (h<sup>-1</sup>) zones, respectively  $A_r$  and  $A_d$  are area of the cross section of the riser (0.0062 m<sup>2</sup>) and area of the cross section of the downcomer (0.0148 m<sup>2</sup>), respectively.

Thus, the  $k_L a(CO_2)_T$  value (downcomer + riser) was obtained for the three spargers and the five air volumetric flows.

### ***Chlorella vulgaris* pre-culture**

*Chlorella vulgaris* strain belonged to the UPI-BI-IPN collection, it was maintained in Petri dishes of solid BBM media. From those Petri dishes, a pre-culture of the algae strain was obtained in a 500-mL flask with 100 mL of BBM media. 100 mL of this pre-cultured biomass was used to inoculate 2-L bottles. The 2-L bottles were grown at a constant temperature of 20±2 °C, irradiation of 100 μmol photons m<sup>-2</sup> s<sup>-1</sup>, and 2 L min<sup>-1</sup> of aeration, with a photoperiod of 12:12 hours, and monitored until an optical density of 0.7 absorbance at 600 nm was obtained (corresponding to 0.15 g L<sup>-1</sup> of biomass). A volume of 1.7 L was used as inoculum for the 17-L PBR.

### Chlorella culture in the airlift bioreactor

The photobioreactor was cleaned and disinfected with sodium hypochlorite. Subsequently, the airlift was rinsed with distilled water to remove residues of the sodium hypochlorite. The disinfection process was performed before starting each of the cultures. The BBM medium was prepared with distilled water (15.3 L) and added to the photobioreactor; finally, 1.7 L of seed culture was added to obtain the operating volume of 17 L in the airlift PBR.

Cultures were run in controlled conditions of temperature ( $20 \pm 2$  °C), irradiation ( $100 \mu\text{mol photons m}^{-2} \text{s}^{-1}$ ), and photoperiod of 12:12 hours. Aeration flows of 9, 17, and  $1.2 \text{ L min}^{-1}$  were employed for all spargers. The cultures of *Chlorella vulgaris* in the PBR were monitored for 15 days.

### Biomass and lipid measurements

Dry biomass concentrations were measured by means of optical density, and converted to dry weight using a calibration curve of optical density versus dry weight, previously obtained. Lipids were measured at the start and end of the cultures, by extraction with hexane, according to Torres *et al.*<sup>23</sup> Biomass and lipid productivities were calculated dividing the maximum biomass (mg dry biomass) or lipids amounts (mg) reached by the day it occurred (days).

### Correlation analysis

The Pearson product or moment correlation coefficient index ( $r^2$ ) was calculated, a dimensionless index between  $-1.0$  and  $1.0$ , inclusive, which reflects the degree of linear dependence between two data sets. For that purpose, the EXCEL 2016 software was employed.

## Results and discussion

### Hydrodynamic characterization

Fig. 2(a) shows the results of mixing time ( $t_M$ ) assessments for different volumetric air flow rates ( $\text{L min}^{-1}$ ). In this work,  $t_M$  is defined as the time needed to reach 90 % of homogeneity in the mixing system<sup>2</sup>. As shown in Fig. 2(a), for the three spargers, the higher air flow rate promoted lower mixing times. This was true for an air flow rate in the range of 5 to  $17 \text{ L min}^{-1}$ . Above this value, the mixing time was higher as the air flow rate increased. This behavior is in agreement with results from the literature. Kojic *et al.*<sup>24</sup> reported that airlifts present three ranges of influence of volumetric air flow rate: 1) uniform bubble flow, Zone I, from 4 to  $9 \text{ L min}^{-1}$ ; 2) transition flow region, Zone II, from 9 to  $17 \text{ L min}^{-1}$ ; and 3) heterogeneous flow, Zone III, above  $17 \text{ L min}^{-1}$ . Data obtained in the present work showed that, in zones I and II, the air flow was low to moderate and the mixing time had reduced as the air flow increased; however, in zone III, the turbulence caused an increase in mixing time as the air flow rate increased. The behavior was rather similar for all three spargers.

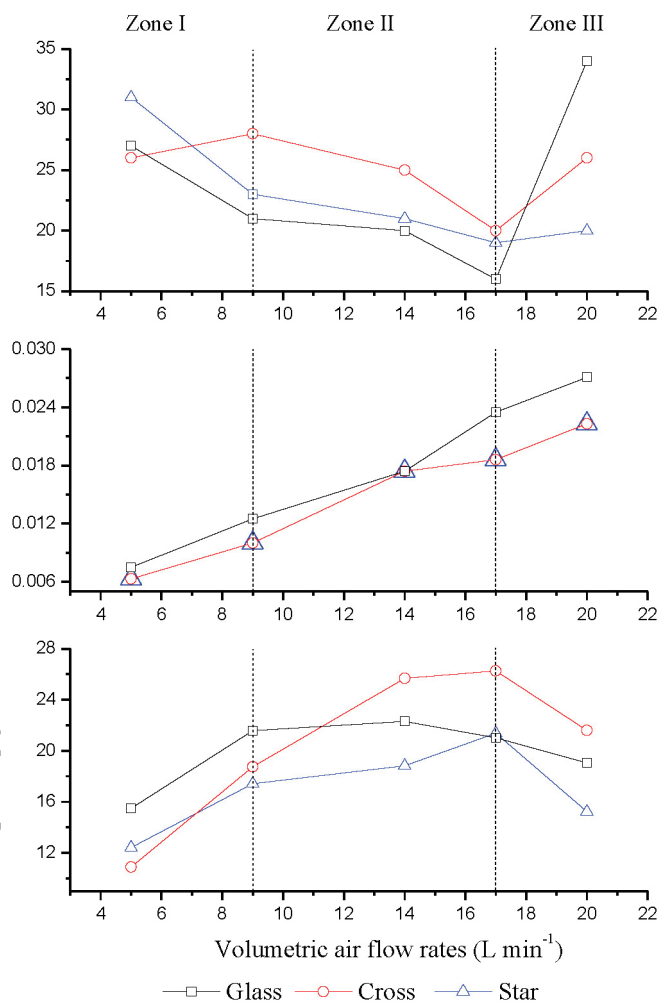


Fig. 2 – a) Mixing time, b) Hold-up, and c)  $k_L a(\text{CO}_2)_r$  as a function of the air flow rate for the different sparger types

from 9 to  $17 \text{ L min}^{-1}$ ; and 3) heterogeneous flow, Zone III, above  $17 \text{ L min}^{-1}$ . Data obtained in the present work showed that, in zones I and II, the air flow was low to moderate and the mixing time had reduced as the air flow increased; however, in zone III, the turbulence caused an increase in mixing time as the air flow rate increased. The behavior was rather similar for all three spargers.

The curves of mixing time versus air flow rate for the star and glass spargers obtained in the present work showed the same tendency as those reported by Oncel<sup>25</sup>. This author determined the mixing times at low air flow rates (up to  $1.5 \text{ L min}^{-1}$ ) for an airlift reactor used for the production of *Chlamydomonas reinhardtii* biomass. The range of air flows employed by Oncel<sup>25</sup> corresponds to the laminar or homogeneous zone. He worked with different riser to downcomer areas ratios ( $A_r/A_d$ ), and the pattern was always the same.

Since the hold-up indicates how much mass can be transferred from the gas to the liquid phase, it is necessary to determine how much of the air fed

Table 1 –  $k_L a(\text{CO}_2)$  values for various airlifts reported in the literature

Photobioreactor	Linear gas speed (m s <sup>-1</sup> )	$k_L a$ (s <sup>-1</sup> )	Reference
Airlift split*	0.001 – 0.009	0.005 – 0.03	22
Concentric tubes airlift	0.0126 – 0.040	0.011 – 0.068	19
Agitated concentric tubes airlift	$U_{gr} < 0.05$	0.0029–0.014	28
Airlift split**	0.024	0.009	34
Airlift external loop**	0.25	0.006	35
Bubbling column**	0.008	0.005	36
Concentric tubes airlift	0.013 – 0.053	0.003 – 0.007	This work

\*flow enriched with 2 % V/V CO<sub>2</sub>, \*\*adapted from Fernandes<sup>22</sup>

into the system is transferred to the liquid phase to allow the growth and metabolic activity of the algae. Fig. 2(b) presents the hold-up values determined for the three different spargers evaluated. In general, data showed that the hold-up values were higher as the air flow rates increased. The results obtained with the stainless steel spargers showed that both behaved similarly (Fig. 2b); therefore, the hold-up for these spargers was practically the same. The glass sparger hold-up values were slightly higher.

The three evaluated spargers showed two inflexion points in the curves of  $t_M$  and  $k_L a(\text{CO}_2)_T$  vs air flow rate, corresponding with the three ranges of influence of volumetric air flow rate, that define zones I to III, respectively. This effect was determined at volumetric air flow rates of 9 and 17 L min<sup>-1</sup>. The change in the slope in the gas hold-up versus the superficial gas velocity is not evident as are the other parameters calculated, as may be seen in Fig. 2(b). This effect could be explained because the data obtained in the present work are similar to those reported by Reyna-Velarde *et al.*<sup>2</sup> Those authors published a curve of mixing time versus linear aeration velocity,  $U_g$ , and found for the range of linear velocities assessed (0.001 to 0.009 m s<sup>-1</sup>), a function of the form  $t_M = 47.2e^{252U_g}$ , with  $r^2 = 0.962$ . According to Kojic *et al.*<sup>24</sup>, the homogeneous regime (bubble flow) occurs at low gas velocities. It is characterized by laminar flow, almost spherical bubbles, lesser bubble-bubble interactions, and the absence of coalescence. Churn turbulent flow occurs at high gas velocities with a strong tendency towards coalescence, with higher rise velocity than smaller bubbles. The transition regime represents the connection between these two patterns. It can be identified also by the change in the slope of the curves. However, in our case, the identification of the zones was determined by calculation of Reynolds number ( $N_R$ ) in circular section ( $N_R = uD/\nu$ ). The  $N_R$  calculation for the riser section involved the gas velocity ( $u$ ) in m s<sup>-1</sup>, the diameter of the riser zone  $D$  equal to 0.089 m, and the kinematic viscosity of the liquid ( $1.02 \cdot 10^{-6}$ ) in m s<sup>-1</sup>. Then, the  $N_R$

values were compared with the standard range of laminar, transition or turbulent zone values<sup>26,27</sup>.

Fig. 2(c) shows the  $k_L a(\text{CO}_2)_T$  values obtained for the range of air flow rates evaluated for the three air spargers. The cross sparger showed the highest  $k_L a(\text{CO}_2)_T$  value of 27 h<sup>-1</sup>, followed by the glass sparger and the star sparger. It is also noticeable that for the star and the cross spargers, the maximum  $k_L a(\text{CO}_2)_T$  value was obtained at a volumetric air flow rate of 17 L min<sup>-1</sup> (at the end of the turbulent zone), whereas for the glass spargers, maximum  $k_L a(\text{CO}_2)_T$  values were observed just at the beginning of the turbulent zone.

The obtained CO<sub>2</sub> values are in the range of  $k_L a$  reported for other systems, such as those summarized in Table 1. For example, the works of Gouveia *et al.*<sup>19</sup> reported  $k_L a$  values in the range of 39.6 – 244.8 h<sup>-1</sup> for a concentric tube airlift with linear gas speeds of 45 – 144 h<sup>-1</sup>. Even in the work of Chisti and Jauregui-Haza<sup>28</sup>, where they used an airlift of concentric tubes with an agitation device,  $k_L a$  values between 10.44 and 50 h<sup>-1</sup> were found, for  $U_{gr} < 0.05$  m s<sup>-1</sup>.

The overall result showed the relationship between air flow, linear velocities, and  $P_g/V$  calculated with Eq. 2. As shown in Table 2, the range of volumetric air flow rates was 5 to 17 L min<sup>-1</sup>, corresponding to linear velocities between 0.013 and 0.053 m s<sup>-1</sup>. The gassing power input per unit of volume ( $P_g/V$ ) ranged from 33 to 134 W m<sup>-3</sup>. These results should be considered in selecting an adequate aeration time and the best sparger to use for this process. Although it is true that the goal of the *Chlorella* culture is to maximize biomass and lipids concentration, the culture energy cost may be excessive for the process.

### *Chlorella vulgaris* growth and productivity

Fig. 3(a) shows the results of *Chlorella* growing in the airlift at the lowest air flow rate (9 L min<sup>-1</sup>) with the three different spargers. The cultures started to grow almost immediately at 8 h. The biomass

Table 2 – Air flow, linear velocities, and specific power input in the airlift

Volumetric air flow (L min <sup>-1</sup> )	Air flow vvm (min <sup>-1</sup> )	Velocity in the riser (m s <sup>-1</sup> )	$P_g/V$ (W m <sup>-3</sup> )
5	0.3	0.013	33
9	0.6	0.025	65
14	0.8	0.036	93
17	1.0	0.046	117
20	1.2	0.053	134

to decline and reached its lowest value (250 mg L<sup>-1</sup>) on day 12. There was a recovery, but high biomass values were no longer determined. On the other hand, the glass and the star spargers promoted higher microalgae concentration, reaching a biomass concentration of 550 and 570 mg L<sup>-1</sup> on day 10. For a medium employing a volumetric air flow rate of 17 L min<sup>-1</sup>, the best spargers were therefore the star and the glass ones.

Finally, when a high volumetric air flow rate (20 L min<sup>-1</sup>) was applied, results were quite different; see Fig. 3(c). At the beginning of the process, the glass sparger seemed to be the best, reaching high biomass values at day 4 (240 mg L<sup>-1</sup>). Nevertheless, from that day on, the biomass started to decline and reached a low biomass at the end of the culture (day 15). The microalgae growth for the cross sparger was slow until day 5, after which the biomass values increased drastically until day 10, achieving a maximum biomass concentration of 700 mg L<sup>-1</sup>. Finally, the star sparger reached the maximum biomass concentration (i.e., 750 mg L<sup>-1</sup>) on day 14.

Biomass productivities were calculated at the time when maximum biomass concentrations had been reached, and the results are summarized in Table 3. The highest biomass productivity was found for the lowest volumetric air flow rate (9 L min<sup>-1</sup>) using the star diffuser; 58.7 mg L<sup>-1</sup> per day were obtained at 8 days of culture. The second highest value was found for the higher volumetric air flow rate (20 L min<sup>-1</sup>) when using the star diffuser. A value of 52.14 mg L<sup>-1</sup> per day was achieved in 14 days. The third best result was obtained for the intermediate value of volumetric air flow rate, 17 L min<sup>-1</sup>, with the star diffuser, reaching 50 mg L<sup>-1</sup> per day in 10 days of *Chlorella* culture.

Results of biomass production are in the range of those previously reported in the literature. Gris *et al.*<sup>29</sup> studied the 11-day growth and lipid production of *Nannochloropsis oculata* in a set of 3.2-L flat-plate airlifts under different conditions. Parameters evaluated were temperature (19 – 29 °C), NaNO<sub>3</sub>

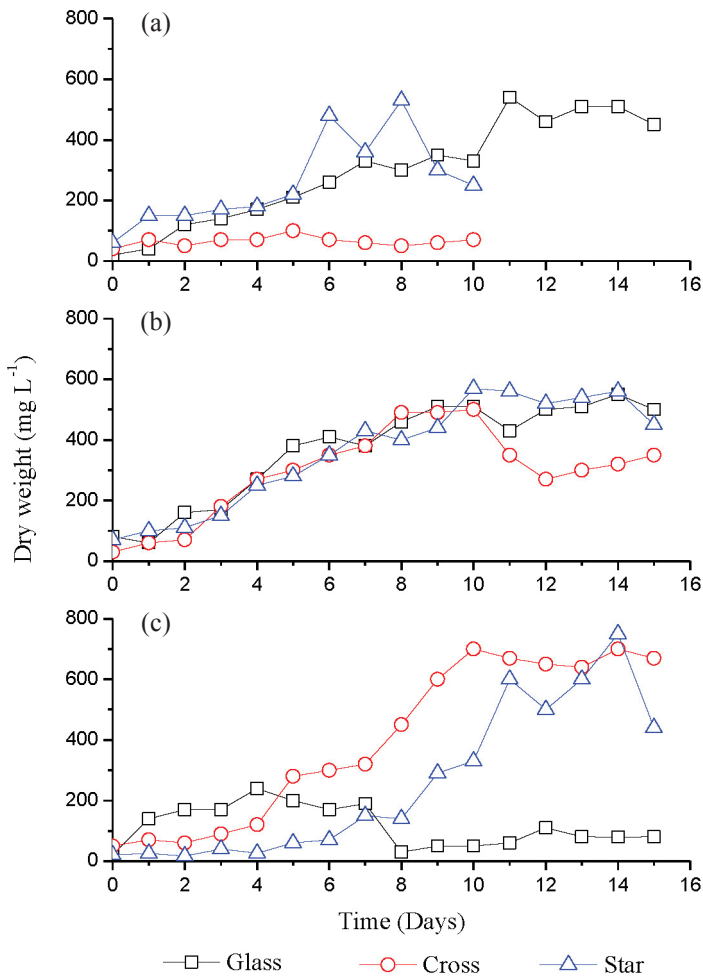


Fig. 3 – Kinetic growth of *Chlorella vulgaris* in the airlift with an air flow rate of a) 0.6 vvm (9 L min<sup>-1</sup>), b) flowrate of 1.0 vvm (17 L min<sup>-1</sup>), and c) 1.2 vvm (20 L min<sup>-1</sup>), and three different spargers

concentration obtained with the cross sparger was always lower than the growth with the other two spargers, and reached quite a low value at day 10 (100 mg L<sup>-1</sup>). At day 5, the culture operated with the star sparger reached higher biomass production, obtaining maximum growth at day 8 (530 mg L<sup>-1</sup>). Finally, the culture carried out using the glass sparger produced higher biomass concentration over a longer period of time, reaching a maximum biomass concentration of 540 mg L<sup>-1</sup> at day 14. These data indicate that when *Chlorella* was grown at low aeration rates, the glass sparger promoted higher biomass production over a longer time.

Fig. 3(b) depicts the *Chlorella* growth at medium volumetric air flow rate of 17 L min<sup>-1</sup> for the three spargers evaluated. There was a lag phase of 1 or 2 days, but after that the three cultures started to grow until day 10, reaching biomass values of around 500 mg L<sup>-1</sup> (as good as the best assessment with a volumetric air flow rate of 9 L min<sup>-1</sup>). From that day on, biomass values changed for the three spargers. The system with the cross sparger started

Table 3 – Summary of the *Chlorella* culture assessments. Effect of sparger type and air flow rate.

Air flow	9 L min <sup>-1</sup>			17 L min <sup>-1</sup>			20 L min <sup>-1</sup>			
	Sparger	Glass	Cross	Star	Glass	Cross	Star	Glass	Cross	Star
$X_{\max}$ (mg L <sup>-1</sup> ) (at day)		540	100	530	550	500	570	240	700	750
		(14)	(5)	(8)	(14)	(10)	(10)	(4)	(14)	(14)
$P_x$ (mg L <sup>-1</sup> d <sup>-1</sup> )		47.27	8	58.75	34	47	50	55	46.43	52.14
$L$ (mg L <sup>-1</sup> )		26	128	13	151	123	7	196	184	10
$P_L$ (mg L <sup>-1</sup> d <sup>-1</sup> )		1.76	8.52	0.87	10	8.22	0.45	13	12.30	0.68
$\mu_{\max}$ (d <sup>-1</sup> )		0.204	ND	0.224	0.269	0.176	0.160	ND	0.302	0.333
Average $\mu_{\max}$ (d <sup>-1</sup> )			0.214			0.201			0.317	

ND = Not determined

concentration (25 – 125 mg L<sup>-1</sup>), and incident light intensity (49 – 140  $\mu\text{mol photons m}^{-2} \text{s}^{-1}$ ). They reported biomass final concentrations between 218 and 482 mg L<sup>-1</sup>.

Mostafa *et al.*<sup>30</sup> reported final dry weight values for the culture of different microalgal strains. More relevant results (flask level) were for *Wolleea saccata* (44.8 mg L<sup>-1</sup>), *Anabaena flos-aquae* (30.08 mg L<sup>-1</sup>), *Chlorella vulgaris* (83.20 mg L<sup>-1</sup>), and *Nostoc humifusum* (47.36 mg L<sup>-1</sup>). Other interesting strains were *Nostoc muscorum* (21.12 mg L<sup>-1</sup>), and *Spirulina platensis* (25.6 mg L<sup>-1</sup>).

### *Chlorella vulgaris* lipid accumulation and productivity

Regarding lipid production (Table 3), the final concentrations were quite different for different aeration regimes, and were also influenced by the type of sparger employed. The highest lipid concentrations were achieved at high volumetric air flow rate (i.e., 20 L min<sup>-1</sup>). The highest lipid concentration was of 196 mg L<sup>-1</sup> for the glass diffuser, followed by the cross sparger (184 mg L<sup>-1</sup>) and the star sparger (only 10 mg L<sup>-1</sup>). For an intermediate aeration rate (17 L min<sup>-1</sup>), results were as follows: the maximum lipid production was found for the glass sparger (151 mg L<sup>-1</sup>), followed by the cross sparger (123 mg L<sup>-1</sup>), and the star sparger (only 7 mg L<sup>-1</sup>). Finally, for the lower aeration rates, lipid production was also lower. The highest value corresponded to the cross sparger (128 mg L<sup>-1</sup>), followed by the glass sparger (26 mg L<sup>-1</sup>), and the star sparger (only 13 mg L<sup>-1</sup>). Maximum lipid productivities were 13, 8.2, and 8.5 mg L<sup>-1</sup> per day for the volumetric air flow rate of 20, 17, and 9 L min<sup>-1</sup>, respectively.

Lipid productivities were quite good in comparison with other works. Zhang and Hong<sup>31</sup> reported the production of 10–50 mg L<sup>-1</sup> of lipids for a *Chlorella* strain growing on sterile or non-sterile wastewater containing around 11 mg L<sup>-1</sup> of TN and 1 mg L<sup>-1</sup> of TP. Mostafa *et al.*<sup>30</sup> reported a lipid pro-

duction in the range of 6.3 to 16.8 mg L<sup>-1</sup> for different strains of microalgae including *Wolleea saccata* (6.3 mg L<sup>-1</sup>) and *Nostoc muscorum* (16.8 mg L<sup>-1</sup>) in wastewater at flask level.

Gris *et al.*<sup>29</sup> studied lipid production of *Nannochloropsis oculata* in a set of 3.2-L flat plate airlifts under different conditions. They reported lipid concentrations between 61.3 and 132.4 mg L<sup>-1</sup>, much lower than those reported in the present work.

Yoo *et al.*<sup>32</sup>, published the study of three different microalgae in order to select one of them to obtain high biomass and lipid productivity. Among the species tested, *Chlorella vulgaris* was evaluated. These authors found the maximum biomass concentration for *Scenedesmus* sp., because this species has a potential ability of C-fixation. The second-best value for biomass productivity was for *Chlorella vulgaris* (104.76 mg L<sup>-1</sup> d<sup>-1</sup>), and finally *Botryococcus braunii*. However, *Botryococcus braunii* was the species with high lipid content for biodiesel production although this species had the lowest biomass productivity. The cultures lasted 14 days, and they were cultivated with ambient air enriched with 2 % CO<sub>2</sub>.

Biomass and lipid production present an inverse correlation, i.e., higher biomass production means lower lipid production. The results showed that under a high aeration rate, the culture of *Chlorella* produced 750 mg L<sup>-1</sup> of biomass when the star sparger was employed, but only 10 mg L<sup>-1</sup> of lipids. In contrast, when the glass sparger was employed, only 240 mg L<sup>-1</sup> of biomass and 196 mg L<sup>-1</sup> of lipids were produced.

Table 3 presents the growth rates calculated for the different *Chlorella* cultures (except for two cases where they were impossible to calculate, due to the erratic disposition of the biomass concentrations). If the average of specific growth rates ( $\mu$ ) for the three spargers is analyzed, it is clear that the high volumetric air flow rate (20 L min<sup>-1</sup>) promoted higher growth rates (0.317 d<sup>-1</sup>), followed by the

lowest volumetric air flow rate (9 L min<sup>-1</sup>) with  $\mu = 0.214$  d<sup>-1</sup>, while the second volumetric air flow rate tested (17 L min<sup>-1</sup>) promoted the lowest average value of  $\mu = 0.201$  d<sup>-1</sup>.

Frumento *et al.*<sup>33</sup> reported the growth of *Chlorella vulgaris* in media containing different concentrations of NaHCO<sub>3</sub> in two different reactor designs: a helicoidal and a horizontal PBR. Results showed that the specific growth rate,  $\mu$ , for the flask experiment was 0.184 d<sup>-1</sup>, while  $\mu$  at reactor values were as high as 0.114 and 0.107 d<sup>-1</sup> for the helicoidal and the horizontal PBRs, respectively. The increment in NaHCO<sub>3</sub> leads to a slight increment in the growth rate (it being 0.289 d<sup>-1</sup> for a NaHCO<sub>3</sub> concentration of 0.2 g L<sup>-1</sup>). More NaHCO<sub>3</sub> induces a decrease in the growth rate again.

Overall results showed that a higher amount of air produced a higher biomass concentration, because more CO<sub>2</sub> was supplied. Air had two main functions inside the airlift: 1) to provide CO<sub>2</sub> for the biomass synthesis, and 2) to promote adequate mixing inside the reactor.

### Correlation analysis

The last goal of this work was to correlate the results of the airlift hydrodynamic characterization with the results of biomass ( $X$ ) and lipid ( $L$ ) concentrations. Pearson coefficient correlations,  $r^2$ , between independent variables ( $P_g/V$ ,  $t_M$ , hold-up, and  $k_L a(\text{CO}_2)_T$ ) with dependent variables ( $X$  and  $L$ ) were carried out. For each sparger, the values of  $X$  and  $L$  correlated fairly well with  $P_g/V$ ,  $t_M$ , hold-up, and  $k_L a(\text{CO}_2)_T$ . The criterion was to select correlations with  $r^2 > 0.8500$ . Specifically, for the glass sparger, good correlations were obtained.

As may be seen in Table 4, both  $X$  and  $L$  values were dependent on  $P_g/V$ ,  $t_M$ , hold-up, and  $k_L a(\text{CO}_2)_T$  for the three spargers, but the best correlations were found for the glass and cross spargers. Regarding  $P_X$  and  $P_L$  productivities, good correlations were observed with  $r^2 > 0.8500$ , but they are not included here since they were calculated based on  $X$  and  $L$  values.

Table 4 – Pearson coefficient correlation,  $r^2$ , calculated for each sparger tested, analyses between independent variables and biomass ( $X$ ) and lipid ( $L$ ) concentrations

Variable \ Sparger	Glass		Cross		Star	
	$X$	$L$	$X$	$L$	$X$	$L$
$P_g/V$	--	0.9931	0.9815	--	--	--
$t_M$	0.9740	--	--	0.9824	--	0.8660
Hold-up	--	0.9998	0.9987	--	--	--
$k_L a(\text{CO}_2)_T$	--	0.9668	0.9958	--	0.8565	--

-- Pearson coefficient correlation ( $r^2$ ) less than 0.8500

### Volumetric gas power input and biomass/lipid productivity

It is important to highlight that, in order to ensure a cost-effective process for biomass and lipids production, the  $P_g/V$  added to the system plays an important role. Therefore, plots of  $P_X$  and  $P_L$  were prepared as a function of  $P_g/V$  calculated values. Fig. 4(a) shows the relationship between  $P_X$  and  $P_g/V$  applied, for the three spargers. It is noticeable that the cross sparger was the most sensitive to the  $P_g/V$  ratio, followed by the glass sparger and the star sparger. On the other hand, the star sparger gave the maximum  $P_X$  values obtained with the minimum  $P_g/V$  cost at the minimum aeration rate. Per day, 58.75 mg L<sup>-1</sup> of biomass can be produced using a  $P_g/V$  of 65 W m<sup>-3</sup>. In contrast, a low  $P_X$  value can be achieved (8 mg L<sup>-1</sup> d<sup>-1</sup>) with the cross sparger, at the same  $P_g/V$  cost.

Fig. 4(b) shows the relationship between  $P_L$  obtained and  $P_g/V$  spent for each of the three spargers. As may be seen, the glass sparger was the most sensitive to the  $P_g/V$  applied, followed by the cross

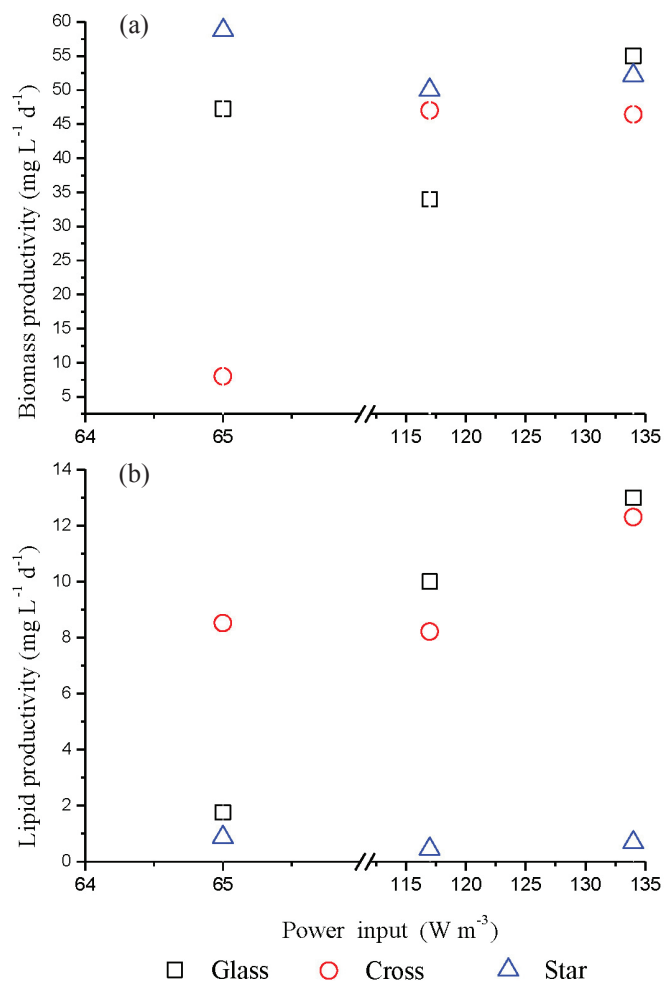


Fig. 4 –  $P_X$  (a) and  $P_L$  (b) as a function of  $P_g/V$  (W m<sup>-3</sup>) for the three spargers

sparger and the star sparger. If the main purpose of the *Chlorella* culture is to obtain the maximum lipids productivity, it is better to use the glass or cross sparger at the maximum aeration rate assessed (with  $P_g/V$  equal to  $133 \text{ W m}^{-3}$ ). By using those spargers,  $P_L$  values 13 and  $12.3 \text{ mg L}^{-1} \text{ d}^{-1}$  can be obtained. Good values of  $P_L$  can be obtained with the cross sparger using the lowest or the medium  $P_g/V$  values (achieving 10 to  $8.22 \text{ mg L}^{-1} \text{ d}^{-1}$ ). The worst performing sparger for achieving  $P_L$  was the star sparger at any aeration rate (values of  $0.45 - 0.87 \text{ mg L}^{-1} \text{ d}^{-1}$ ).

As far as we know, there are no reports of biomass and lipid productivities as a function of air flow rates for different spargers. Only Ying *et al.*<sup>6</sup> compared the performance of two 3-L airlift PBRs (a standard one and the other with a fluidic oscillator) to grow *Dunaliella salina* at  $24 \text{ }^\circ\text{C}$  (volumetric air flow rates were varied between  $0.3$  and  $1.1 \text{ L min}^{-1}$ ). The authors reported a graph of specific growth ( $\text{d}^{-1}$ ) vs. volumetric air flow rate ( $\text{L min}^{-1}$ ) for two different airlift PBRs, with and without the fluidic oscillator. The lines obtained were second-degree polynomials with a maximum volumetric air flow rate of  $0.91 \text{ L min}^{-1}$ , with values of  $0.17 \text{ d}^{-1}$  for the airlift with the fluidic oscillator and  $0.13 \text{ d}^{-1}$  for the standard one. The authors concluded that algal growth might be correlated to mass transfer, specifically because the airlift with the fluidic oscillator was capable of giving better  $k_L a(\text{CO}_2)$  values, and maintaining higher dissolved  $\text{CO}_2$  concentrations.

## Conclusions

The results obtained in the present work showed the key effect of the type of sparger and air flow rate on the hydrodynamic behavior of the airlift reactor and the algae biological process. Thus, the data of biomass concentration could be summarized as changes in the air flow and sparger type, as follows: when *Chlorella* was grown at low aeration rates ( $9 \text{ L min}^{-1}$ ), the glass sparger promoted higher biomass production for a longer time. For a medium volumetric air flow rate ( $17 \text{ L min}^{-1}$ ), the star and glass spargers were the best-performing. Whereas, when a high volumetric air flow rate ( $20 \text{ L min}^{-1}$ ) was applied, the star sparger reached the maximum biomass concentration.

Regarding the biomass productivity, the highest value was found at the lowest aeration rate using the star diffuser. A productivity of  $58.7 \text{ mg L}^{-1} \text{ d}^{-1}$  was determined in 8 days of culture. The second-best value was found for the higher aeration rate when using the star diffuser. A value of  $52.14 \text{ mg L}^{-1} \text{ d}^{-1}$  was achieved in 14 days. The third-best

result was observed for the medium aeration rate with the star diffuser, reaching  $50 \text{ mg L}^{-1} \text{ d}^{-1}$  in 10 days of *Chlorella* culture.

The highest lipid concentration of  $196 \text{ mg L}^{-1}$  was achieved at high aeration rates ( $20 \text{ L min}^{-1}$ ) for the glass diffuser, followed by the cross sparger ( $184 \text{ mg L}^{-1}$ ) and finally, the star sparger ( $10 \text{ mg L}^{-1}$ ). For intermediate aeration rates, the results obtained were as follows: the maximum lipid concentration was found for the glass sparger as well ( $151 \text{ mg L}^{-1}$ ), followed by the cross sparger ( $123 \text{ mg L}^{-1}$ ) and the star sparger ( $7 \text{ mg L}^{-1}$ ). For lower aeration rates, lipid concentration was generally lower. The highest value corresponded to the cross sparger ( $128 \text{ mg L}^{-1}$ ) followed by the glass sparger ( $26 \text{ mg L}^{-1}$ ) and the star sparger ( $13 \text{ mg L}^{-1}$ ). Maximum lipid productivities of 13, 8.2, and  $8.5 \text{ mg L}^{-1}$  per day were observed for the volumetric air flow rates of 9, 17, and  $20 \text{ L min}^{-1}$ , respectively.

Under a high aeration rate, the *Chlorella* culture produced  $750 \text{ mg L}^{-1}$  of biomass when the star sparger was used, but only  $10 \text{ mg L}^{-1}$  of lipids. On the other hand, when the glass sparger was employed, only  $240 \text{ mg L}^{-1}$  of biomass and  $196 \text{ mg L}^{-1}$  of lipids were produced. Thus, if the main purpose of the *Chlorella* culture is to obtain the maximum productivity of lipids, it will be worth using star or cross spargers at the maximum aeration rate assessed.

## ACKNOWLEDGEMENTS

We thank CONACYT for Y. Lopez-Hernandez's scholarship. Authors thank J. Martinez-Limon (UP-IBI-IPN) for his support for  $k_L a$  calculations. The economic support of the IPN through 20160635 Grant is appreciated.

## Nomenclature

$A_d$	– area of the cross-section of the downcomer, $\text{m}^2$
$A_r$	– area of the cross-section of the riser, $\text{m}^2$
$\gamma$	– concentration of dissolved oxygen at a given time ( $t$ ), $\text{mg L}^{-1}$
$\gamma_0$	– dissolved oxygen concentration at zero time ( $t_0$ ), $\text{mg L}^{-1}$
$\gamma^*$	– saturation concentration of dissolved oxygen, $\text{mg L}^{-1}$
$D_{\text{CO}_2}$	– diffusion coefficient of carbon dioxide, $\text{m s}^{-2}$
$D_{\text{O}_2}$	– oxygen diffusion coefficient, $\text{m s}^{-2}$
$g$	– acceleration of gravity, $\text{m s}^{-2}$
$H$	– height of liquid unaerated, $\text{m}$
$H_G$	– gassed liquid height, $\text{m}$
$H_L$	– height of still liquid without aerating, $\text{m}$

$k_L a_r$	– volumetric mass transfer coefficient of the riser area, $\text{h}^{-1}$
$k_L a_d$	– volumetric mass transfer coefficient of the downcomer zone, $\text{h}^{-1}$
$k_L a(\text{CO}_2)$	– volumetric mass transfer coefficient of $\text{CO}_2$ , $\text{h}^{-1}$
$k_L a(\text{O}_2)$	– volumetric mass transfer coefficient of oxygen, $\text{h}^{-1}$
$k_L a(\text{CO}_2)_T$	– total volumetric mass transfer coefficient of carbon dioxide, riser, and downcomer, $\text{h}^{-1}$
$L$	– lipids concentration at the end of kinetic growth, $\text{mg L}^{-1}$
$p_a$	– head pressure, Pa
$P_g/V$	– power supplied by gas, per volume unit, $\text{W m}^{-3}$
$P_X$	– biomass productivity, $\text{mg L}^{-1} \text{d}^{-1}$
$P_L$	– lipid productivity, $\text{mg L}^{-1} \text{d}^{-1}$
$Q_m$	– molar flow of air, $\text{mol s}^{-1}$
$R$	– gas constant, $\text{J mol}^{-1} \text{K}^{-1}$
$T$	– temperature, K
$t_M$	– mixing time, s
$t_0$	– zero time, $\text{h}^{-1}$
$U_g$	– superficial gas velocity, $\text{m s}^{-1}$
$V_L$	– operating volume of the reactor, $\text{m}^3$
$X$	– biomass concentration at the end of kinetic growth, $\text{mg L}^{-1}$
$X_{\text{max}}$	– maximum biomass, $\text{g L}^{-1}$

### Greek symbols

$\varepsilon$	– hold-up, dimensionless
$\rho$	– density of the liquid, $\text{kg m}^{-3}$
$\mu_{\text{max}}$	– maximum specific growth rate, $\text{d}^{-1}$

### Abbreviations

ALB	– Airlift photobioreactor
BBM	– Bold Basal Media
PBR	– Photobioreactor

### References

- Olivieri, G., Salatino, P., Marzocchella, A., Advances in photobioreactors for intensive microalgal productions: Configurations, operating strategies and applications, *J. Chem. Technol. Biotechnol.* **894** (2013) 178.
- Reyna-Velarde, R., Cristiani-Urbina, E., Hernández-Melchor, D. J., Thalasso, F., Cañizares-Villanueva, R. O., Hydrodynamic and mass transfer characterization of a flat-panel airlift photobioreactor with high light path, *Chem. Eng. Process.* **49** (2010) 97. doi: <https://doi.org/10.1016/j.cep.2009.11.014>
- Kumar, K., Das, D., Growth characteristics of *Chlorella sorokiniana* in airlift and bubble column photobioreactors, *Biores. Technol.* **116** (2012) 307. doi: <https://doi.org/10.1016/j.biortech.2012.03.074>
- Rengel, A., Zoughaib, A., Dron, D., Clodic, D., Hydrodynamic study of an internal airlift reactor for microalgae culture, *Appl. Microbiol. Biotechnol.* **93** (2012) 117. doi: <https://doi.org/10.1007/s00253-011-3398-9>
- Münkel, R., Schmid-Staiger, U., Werner, A., Hirt, T., Optimization of outdoor cultivation in flat panel airlift reactors for lipid production by *Chlorella vulgaris*, *Biotechnol. Bioeng.* **110** (2013) 2882. doi: <https://doi.org/10.1002/bit.24948>
- Ying, K., Al-Mashhadani, A. K. H., Hanotu, J. O., Gilmour, D. J., Zimmerman, W. B., Enhanced mass transfer in micro-bubble driven airlift bioreactor for microalgae culture, *Engineering* **5** (2013) 735. doi: <https://doi.org/10.4236/eng.2013.59088>
- Vunjak-Novakovic, G., Kim, Y., Wu, X., Berzin, I., Merchuk, J. C., Air-lift bioreactors for algal growth on flue gas: Mathematical modeling and pilot plant studies, *Ind. Eng. Chem. Res.* **44** (2005) 6154. doi: <https://doi.org/10.1021/ie049099z>
- Yun, Y. S., Park J. M., Attenuation of monochromatic and polychromatic lights in *Chlorella vulgaris* suspensions, *Appl. Microbiol. Biotechnol.* **55** (2001) 765. doi: <https://doi.org/10.1007/s002530100639>
- Cabello, J., Morales, M., Revah, S., Dynamic photosynthetic response of the microalga *Scenedesmus obtusiusculus* to light intensity perturbations, *Chem. Eng. J.* **252** (2014) 104. doi: <https://doi.org/10.1016/j.cej.2014.04.073>
- Deckwer, W.-D., Schumpe, A., Improved tools for bubble column reactor design and scale-up, *Chem. Eng. Sci.* **51** (1993) 889. doi: [https://doi.org/10.1016/0009-2509\(93\)80328-N](https://doi.org/10.1016/0009-2509(93)80328-N)
- Kulkarni, A. A., Joshi, J. B., Bubble formation and bubble rise velocity in gas-liquid systems: A review, *Ind. Eng. Chem. Res.* **44** (2005) 5873. doi: <https://doi.org/10.1021/ie049131p>
- Ugwu, C. U., Aoyagi, H., Uchiyama, H., Photobioreactors for mass cultivation of algae, *Bioresour. Technol.* **99** (2008) 4021. doi: <https://doi.org/10.1016/j.biortech.2007.01.046>
- Robles-Heredia, J. C., Narváez-García, A., Ruiz-Marin, A., Canedo-Lopez, Y., Zavala-Loria, J. C., Sacramento-Rivero, J. C., in: Effect of Hydrodynamic Conditions of Photobioreactors on Lipids Productivity in Microalgae, *IntechOpen*, 2018, pp 39-57.
- Chisti, Y., Airlift Bioreactors, Elsevier Applied Science, London, UK, 1989. pp 1-349.
- Chisti, Y., Jauregui-Haza, U. J., Microalgal production and mass transfer characterization in a vertical flat-plate photobioreactor, *Bioprocess Biosyst. Eng.* **25** (2002) 97. doi: <https://doi.org/10.1007/s00449-002-0284-y>
- Carvalho, A. P., Meireles, L. A., Malcata, F. X., Microalgal reactors: A review of enclosed system designs and performances, *Biotechnol. Prog.* **22** (2006) 1490. doi: <https://doi.org/10.1002/bp060065r>
- Chisti, Y., Moo-Young, M., Hydrodynamics and oxygen transfer in pneumatic bioreactor devices, *Biotechnol. Bioeng.* **31** (1988) 487. doi: <https://doi.org/10.1002/bit.260310514>
- Shamlou, P. A., Pollard, D. J., Ison, A. P., Volumetric mass transfer coefficient in concentric-tube airlift bioreactors, *Chem. Eng. Sci.* **50** (1995) 1579. doi: [https://doi.org/10.1016/0009-2509\(94\)00517-U](https://doi.org/10.1016/0009-2509(94)00517-U)

19. *Gouveia, E. R., Hokka, C. O., Badino-Jr, A. C.*, The effects of geometry and operational conditions on gas hold up, liquid circulation and mass transfer in airlift reactor, *Braz. J. Chem. Eng.* **20** (2003) 363.  
doi: <https://doi.org/10.1590/S0104-66322003000400004>
20. *Fadavi, A., Chisti, Y.*, Gas hold up and mixing characteristics of a novel forced circulation loop reactor, *Chem. Eng. J.* **131** (2006) 105.  
doi: <https://doi.org/10.1016/j.cej.2006.12.037>
21. *Moutafchieva, D., Popova, D., Dimitrova, M., Tchaoushev, S.*, Experimental determination of the volumetric mass transfer coefficient, *J. Chem. Tech. Metal.* **48** (2013) 351.
22. *Fernandes, B. D., Mota, A., Ferreira, A., Dragone, G.*, Characterization of split cylinder airlift photobioreactor for efficient microalgae cultivation, *Chem. Eng. Sci.* **117** (2014) 445.  
doi: <https://doi.org/10.1016/j.ces.2014.06.043>
23. *Torres, L. G., Martinez, M., Garcia, J. D., Fernandez, L. C.*, Three microalgae strains culture using human urine and light, *J. Chem. Biol. Phys. Sci.* **4** (2014) 74.
24. *Kojic, P. S., Tokic, M. S., Sijacki, I. M., Lukic, N. Lj.*, Influence of the sparger type and added alcohol on the gas hold up of an external loop airlift reactor, *Chem. Eng. Technol.* **38** (2015) 701.  
doi: <https://doi.org/10.1002/ceat.201400578>
25. *Oncel, S.*, Focusing on the optimization for scale up in airlift bioreactors and the production of *Chlamydomonas reinhardtii* as a model microorganism, *Ekoloji.* **23** (2014) 20.  
doi: <https://doi.org/10.5053/ekoloji.2014.903>
26. *Mott, R. L.*, *Fluid Mechanics*, Prentice Hall, México, 2006, pp 230-231.
27. *Geankopolis, C. J.*, *Transport Processes and Separation Process Principles (including Unit Operations)*, Patria Editorial Group, México, 2008., pp 52–54.
28. *Chisti, Y., Jauregui-Haza, U. J.*, Oxygen transfer and mixing in mechanically agitated airlift bioreactors, *Biochem. Eng. J.* **10** (2002) 143.  
doi: [https://doi.org/10.1016/S1369-703X\(01\)00174-7](https://doi.org/10.1016/S1369-703X(01)00174-7)
29. *Gris, L. R. S., Paim, A. C., Farenzena, M., Trierweiler, J. O.*, Laboratory apparatus to evaluate microalgae production, *Braz. J. Chem. Eng.* **30** (2013) 487.  
doi: <https://doi.org/10.1590/S0104-66322013000300007>
30. *Mostafa, S. S. M., Shalaby, E. A., Mahmoud, G. I.*, Cultivating microalgae in domestic wastewater for biodiesel production, *Nat. Sci. Biol.* **4** (2012) 56.  
doi: <https://doi.org/10.15835/nsb417298>
31. *Zhang, Q., Hong, Y.*, Comparison in growth, lipid accumulation and nutrient removal capacities of *Chlorella* sp. in secondary effluents under sterile and non-sterile conditions, *Water Sci. Tech.* **69** (2014) 573.  
doi: <https://doi.org/10.2166/wst.2013.748>
32. *Yoo, C., Jun, S., Lee, J., Ahn, C., Oh, H.*, Selection of microalgae for lipid production under high levels carbon dioxide, *Bioresour. Tech.* **101** (2010) S71.  
doi: <https://doi.org/10.1016/j.biortech.2009.03.030>
33. *Fruemento, D., Casazza, A. A., Al-Arni, S., Converti, A.*, Cultivation of *Chlorella vulgaris* in tubular photobioreactors: A lipid source for biodiesel production, *Biochem. Eng. J.* **81** (2013) 120.  
doi: <https://doi.org/10.1016/j.bej.2013.10.011>
34. *Vega-Estrada, J., Montes-Horcasitas, M. C., Dominguez-Bocanegra, A. R., Cañizares Villanueva, R. O., Haematococcus pluvialis* cultivation in split-cylinder internal loop airlift photobioreactor under aeration conditions avoiding cell damage, *Appl. Microbiol. Biotechnol.* **68** (2005) 31.  
doi: <https://doi.org/10.1007/s00253-004-1863-4>
35. *Acien Fernandez, F. G., Fernández Sevilla, J. M., Sánchez Pérez, J. A., Molina Grima, E., Chisti, Y.*, Airlift-driven external-loop tubular photobioreactors for outdoor production of microalgae: Assessment of design and performance, *Chem. Eng. Sci.* **56** (2001) 2721.  
doi: [https://doi.org/10.1016/S0009-2509\(00\)00521-2](https://doi.org/10.1016/S0009-2509(00)00521-2)
36. *Merchuk, J. C., Gluz, M., Mukmenev, I.*, Comparison of photobioreactors for cultivation of the red microalga *Porphyridium* sp., *J. Chem. Technol. Biotechnol.* **75** (2000) 1119.  
doi: [https://doi.org/10.1002/1097-4660\(200012\)75:12<1119::AID-JCTB329>3.0.CO;2-G](https://doi.org/10.1002/1097-4660(200012)75:12<1119::AID-JCTB329>3.0.CO;2-G)